JOURNAL OF PHYSICAL ORGANIC CHEMISTRY
J. Phys. Org. Chem. 2000: **13;** 46–56

Contrasting mechanism of the hydration of carbon suboxide and ketene. A theoretical study†

Minh Tho Nguyen,* Greet Raspoet and Luc G. Vanquickenborne

Department of Chemistry, University of Leuven, Celestijnenlaan 200F, B-3001 Leuven, Belgium

Received 8 February 1999; revised 16 June 1999; accepted 19 June 1999

ABSTRACT: The protonation and hydration of carbon suboxide (O=C=C=C=O) were studied by *ab initio* molecular orbital methods. While the geometries of the stationary points were optimized using MP2/6–31G(d,p) calculations, relative energies were estimated using QCISD(T)/6–31G(d,p) and 6–311++G(d,p) + ZPE. The behaviour of carbon suboxide was compared with that of carbon dioxide and ketene. The protonation at the β-carbon is consistently favoured over that at the oxygen; the proton affinities (*PA*) are estimated to be $PA(C_3O_2) = 775 \pm 15$ and $PA(H_2CCO) = 820 \pm 10$ kJ mol^{-1} (experimental: 817 ± 3 kJ mol^{-1}). The *PA*s at oxygen amount to 654, 641 and 542 kJ mol^{-1} (experimental: 548 kJ mol^{-1}) for C_3O_2, H_2CCO and CO_2, respectively. Using the approach of one and two water molecules to model the hydration reaction, the calculated results consistently show that the addition of water across the C=O bond of ketene, giving a 1,1-ethenediol intermediate, is favoured over the C=C addition giving directly a carboxylic acid. A reverse situation occurs in carbon suboxide. In the latter, the energy barrier of the C=C addition is about 31 kJ mol^{-1} smaller than that of C=O addition. The C=C addition in C_3O_2 is inherently favoured owing to a smaller energetic cost for the molecular distortion at the transition state, and a higher thermodynamic stability of the acid product. Molecular deformation of carbon suboxide is in fact a fairly facile process. A similar trend was observed for the addition of H_2, HF and HCl on C_3O_2. In all three cases, the C=C addition is favoured, HCl having the lowest energy barrier amongst them. These preferential reaction mechanisms could be rationalized in terms of Fukui functions for both nucleophilic and electrophilic attacks. Copyright © 2000 John Wiley & Sons, Ltd.

KEYWORDS: carbon suboxide; carbon dioxide; ketene; hydration mechanism; protonation; *ab initio* calculations; Fukui functions

INTRODUCTION

Carbon suboxide (**1**) (O=C=C=C=O) was first prepared at the beginning of this century[1] and its chemistry has received continuing interest.[2] This higher oxide of carbon belongs to the family of cumulenones which includes among others, methyleneketene (H_2C=C=C=O). In some regards, carbon suboxide (C_3O_2) can also be classified as a bisketene.[3] In atmospheric and combustion chemistry, **1** is often employed as a fuel and in atomic oxygen flames as a source of triplet carbon monoxide (CO).[4] The presence of C_3O_2 on Halley's comet has also been proposed.[5] As water ice is the main component on this comet,[6] hydration of **1** could be expected to be a primary transformation. It is known that this reaction gives the bis-acid **2** as the final product:[7]

$$\underset{\mathbf{1}}{O{=}C{=}C{=}C{=}O} + 2H_2O \rightarrow \underset{\mathbf{2}}{H_2C(CO_2H)_2} \qquad (1)$$

Recently, Allen *et al.*[8] measured rate constants for reaction of **1** in a mixture of water and acetonitrile by monitoring their UV spectra. The fact that only a single rate process was observed, irrespective of the water percentage, indicates an initial addition of water to one ketene function of **1**. It has been found[8] that the hydration rate of C_3O_2 is substantial but lower than that of ketene [H_2C=C=O (**3**)] by factors of 2.5×10^3 in neutral conditions and 5.2×10^4 for the acid-catalysed reaction.[7] In fact, Staudinger and Bereza[1c] observed that carbon suboxide was stable in the presence of alcohols for prolonged periods at low temperatures. To assist the interpretation of kinetic results, some *ab initio* molecular orbital calculations at the MP2/6–31G(d,p) level have been carried out.[8] Accordingly, the most favoured

**Correspondence to:* M. T. Nguyen, Department of Chemistry, University of Leuven, Celestijnenlaan 200F, B-3001 Leuven, Belgium. E-mail: minh.nguyen@chem.kuleuven.ac.be

† Dedicated to our colleague and friend, José Elguero, on the occasion of his 65th birthday.

Contract/grant sponsor: FWO-Vlaanderen.
Contract/grant sponsor: IWT-Vlaanderen.
Contract/grant sponsor: GOA-program, KU Leuven.

CCC 0894–3230/2000/010046–11 $17.50

protonation of C_3O_2 occurs at the central carbon whereas the keto acid form [O=C=CHCOOH **(4)**] is much more stable than its diol isomer [O=C=C=C(OH)$_2$ (**5**)]. This is similar to the behavior of ketene regarding protonation and hydration product.[10,11] Nevertheless, it has also been well established both theoretically[11–15] and experimentally[15–18] that the preferential hydration of ketene **3** is a two-step process involving an addition of water across its C=O bond followed by a conversion of the 1,1-ethenediol intermediate **6** to the more stable acetic acid **7**:

$$\underset{\mathbf{1}}{H_2C{=}C{=}O} + H_2O \rightarrow \underset{\mathbf{6}}{H_2C{=}C(OH)_2} \rightarrow \underset{\mathbf{7}}{H_3CCOOH} \quad (2)$$

The one-step addition of water across the C=C bond of **3** giving **7** directly has been found to require a slightly larger activation energy.[15] In some substituted cases, the ethenediol has been detected spectrometrically.[18] On the basis of the fact that the isotope effects are similar in both neutral hydrations of C_3O_2 and ketene, $k(H_2O)/k(D_2O) = 2.2$ and 1.6–1.8, respectively, Allen *et al.*[8] suggested that both reactions involve the same mechanism, namely via a diol intermediate. Nevertheless, these authors were not successful in locating the transition structures associated with both C=C and C=O additions using MO calculations. Therefore, the question as to whether or not the hydration of **1** involves **5** remains open:

$$\underset{\mathbf{1}}{O{=}C{=}C{=}C{=}O} + H_2O \rightarrow \underset{\mathbf{5}}{O{=}C{=}C{=}C(OH)_2} \rightarrow \underset{\mathbf{6}}{O{=}C{=}CHCOOH} \quad (3)$$

In this work, we have attempted to tackle this question with the aid of molecular orbital calculations. As demonstrated in earlier studies,[13–15,19–21] the attack of water on a double bond is better modelled by, at least, two water molecules that participate fully in the reacting supersystem. In fact, the second water molecule acts as a bifunctional catalyst facilitating the proton transfer. Therefore, we have considered in this work the addition of water monomer and water dimer across both C=O and C=C bonds of carbon suboxide. For the purpose of comparison, results obtained using the same approach are also given here for the hydration of ketene[21a] and carbon dioxide,[22] in addition to the protonation at both carbon and oxygen centres. Finally, the additions of H_2, HCl and HF to C_3O_2 were also compared with that of water.

METHODS OF CALCULATION

Ab initio MO calculations were carried out using a local version of the Gaussian 94 set of programs.[23] One-electron basis functions including the 6–31G(d,p) and 6–311 ++G(d,p) sets were employed. The potential energy surfaces were initially mapped out using the Hartree–Fock (HF) method in conjunction with the 6–31G(d,p) basis, and the located structures were characterized by harmonic vibrational analyses at this level. Geometric parameters of the relevant equilibrium and transition-state structures were subsequently re-optimized at a higher level of theory partly incorporating electron correlation, namely the second-order perturbation theory MP2/6–31G(d,p). Thermochemical parameters were then determined by single-point electronic energies computed using the quadratic configuration interaction method, QCISD(T), using MP2-optimized geometries with the basis sets mentioned above. Hence the choice of a basis set for a system is mainly determined by the capacity of our computing resources. In MP2 and QCI calculations, the core orbitals were kept frozen. In order to predict the reactive behaviour of a molecule, the molecular electrostatic potential (MEP) was used, defined as the interaction energy of the molecule with a positive point charge placed at position *r*. Moreover, Fukui functions for both nucleophilic and electrophilic attacks were calculated using the finite difference approximation introduced by Parr and Yang.[24] Hence the Fukui function, which is given by the expression

$$f(\mathbf{r}) = \left.\frac{\partial \rho(\mathbf{r})}{\partial N}\right|_{\nu(\mathbf{r})}$$

is computed as follows:

$$f^{(+)}(r) = \rho(N+1) - \rho(N)$$

$$f^{(-)}(r) = \rho(N) - \rho(N-1)$$

where $\rho\ (N+1)$, $\rho\ (N)$ and $\rho\ (N-1)$ are the electron densities of the $N+1$, N and $N-1$ electron systems respectively, all calculated at the geometries of the N electron systems. These calculations were performed using the B3PW91 functionals combined with the correlation-consistent cc-pVTZ basis set which has already been proved to be successful[25] and the (U)MP2/6–31G(d,p) wavefunctions. As UHF wavefunctions of open-shell cations and anions, which are needed in the calculations of Fukui functions, are contaminated by higher spin states, the corresponding UMP2 energies often suffer from a slow convergence of the perturbation expansion. In this case, the DFT method clearly presents an advantage over the MO method in not having a severe spin contamination problem. In addition, for the sake of comparison with earlier results[21,25] only the plots computed using B3PW91 calculations are reported in this paper. Whereas $f^{(+)}$ is an indicator for nucleophilic attack, $f^{(-)}$ is an indicator for electrophilic attack.

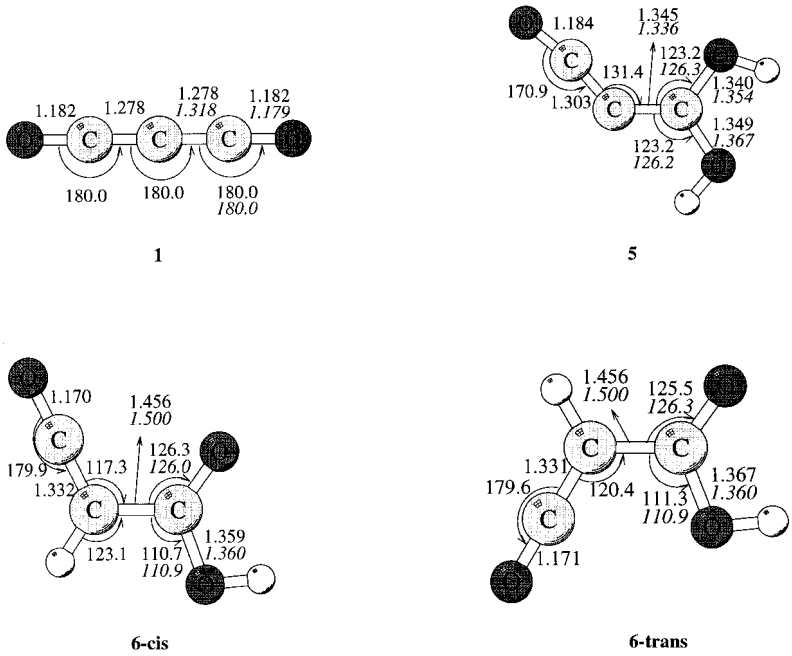

Figure 1. MP2/6–31G(d,p)-optimized geometries of the equilibrium structures. Values given in italics correspond to those of ketene

Throughout this paper, unless noted, otherwise total energies are given in hartrees, relative and zero-point energies in kJ mol^{-1}, bond lengths in angströms and bond angles in degrees.

RESULTS AND DISCUSSION

Properties of carbon suboxide

The carbon suboxide species is calculated to have a strictly symmetrical and linear framework, as shown by a vibrational analysis at the MP2/6–31G(d,p) level. Note that the analogous propadienone ($H_2C{=}C{=}C{=}O$) possesses a non-linear heavy-atom chain.[26] The free molecule shows a typical IR absorption band at 2289 cm^{-1} in a argon matrix.[27,28] After scaling the MP2/6–31G(d,p) harmonic vibrational wavenumbers by an average factor of 0.95, the calculated values are 114, 550, 552, 740, 1537, 2141 and 2366 cm^{-1}. The absorption at 2366 cm^{-1} can be compared with the experimental value and corresponds to a C=O antisymmetric stretching mode. Concerning the geometry, the C=O distance in **1** is similar to that in O=C=O and $H_2C{=}C{=}O$ whereas the C=C distance is shorter than that in $H_2C{=}C{=}O$, which is no doubt due to a multiple cumulene structure (Fig. 1). Roughly speaking, this bond is formed from two sp-hybridized carbons in **1** but from both sp and sp^2 carbons in ketene; therefore, the former is a shorter bond.

Table 1. Calculated proton affinities (kJ mol^{-1}) of carbon suboxide, carbon dioxide and ketene

	C-protonation		O-protonation		
Method[a]	C_3O_2	H_2CCO	C_3O_2	H_2CCO	OCO
MP2/6–31G(d,p)	783	851	655	644	544
QCISD(T)/6–31G(d,p)	801	851	669	667	554
CCSD(T)/6–31G(d,p)[b]	—	—	—	—	555
QCISD(T)/6–311++G(d,p)	785	836	654	646	545
QCISD(T)/6–311++G(3df,2p)	—	820	—	641	535
CCSD(T)/6–311++G(3df,2p)[b]	—	—	—	—	542
Exptl	—	817[c], 825[d]	—	—	536[e], 548[d]

[a] At the indicated level including ZPE corrections, based on MP2/6–31G(d,p) geometries unless noted otherwise.
[b] Based on CCSD(T)-optimized geometries
[c] Ref. 31.
[d] Ref. 29.
[e] Ref. 30.

Table 2. Calculated total and relative energies of the points of interest on the addition path of one water molecule to C_3O_2

Structure[a]	ZPE[b]	MP2/6–31G(d,p)	QCISD(T)/6–31G(d,p)	Relative energies[c]	
				MP2	QCISD(T)
C_3O_2 (**1**)	56	−264.02793	−264.03519	—	—
H_2O	55	−76.22245	−76.23166	—	—
$C_3O_2 + H_2O$	111	−340.25038	−340.26685	0	0
$OCCC(OH)_2$ (**5**)	128	−340.23936	−340.26201	46	29
OCCH-COOH (**6**- *cis*)	125	−340.28833	−340.31256	−85	−106
OCCH-COOH (**6**- *trans*)	126	−340.28806	−340.31230	−84	−105
TS C=O (**TS1/CO**)	112	−340.16813	−340.18716	217	210
TS C=C (**TS1/CC**)	110	−340.18567	340.20390	169	164

[a] Based on MP2/6–31G(d,p) geometries.
[b] From HF/6–31G(d,p) calculations and scaled by 0.9.
[c] At the indicated level with the 6–31G(d,p) basis and corrected for ZPEs.

The stability of various protonated forms is an indicator for the acid-catalysed reaction. As mentioned above, the C_β protonation in **1** and ketene is largely favoured over O protonation (in carbon dioxide the protonation occurs at the oxygen atom). The proton affinity (*PA*) of the latter has been repeatedly determined by different spectroscopic techniques.[29,30] Calculated *PA*s using different theoretical methods are given in Table 1. It is obvious that the difference between both C_β and O *PA*s is strongly reduced on going from ketene to carbon suboxide, presumably owing to the higher stability of the resulting CH_3CO^+ cation. On the other hand, *PA*(O) increases in the sequence $CO_2 < H_2CCO < C_3O_2$. The results in Table 1 indicate that good agreement with experiment is possible, as can be achieved for both ketene and CO_2 molecules when using large basis sets. At the QCISD(T)/6–311++G(d,p) level, which is the highest level available here for C_3O_2, the computed *PA*s for the CH_2CO or CO_2 are overestimated by about 10 kJ mol^{-1} compared with the most recent experimental determinations. Taking this correction into account, we would propose a proton affinity for carbon suboxide of $PA(C_3O_2)$ = 775 kJ mol^{-1}, with a probable error of ± 15 kJ mol^{-1}.

Relative stability between ethenediol and carboxylic acid products

Calculated results are given in Table 2. Whereas the diol **5** is the product of a C=O addition of water to **1**, the ketenyl acid **6** is the C=C adduct (cf. Fig. 1). The conformations of this class of compounds have been analysed in detail in earlier studies.[32,33] Our calculations show that both conformers **6-*cis*** and **6-*trans*** have a similar energy content and are connected to each other by an energy barrier for rotation of about 50 kJ mol^{-1}. In agreement with earlier studies,[8] the acid **6** is about 135 kJ mol^{-1} more stable than the diol **5**. At the same level of theory, the energy difference between 1,1-ethenediol [$H_2C=C(OH)_2$] and acetic acid (CH_3COOH) amounts to 134 kJ mol^{-1}. Hence the energy variation due to the cumulene structure present in the **5–6** pair is not significantly large. Note that for the pair of ethenediol–acetic acid isomers, higher level calculations[11] suggested an energy difference of 115 ± 10 kJ mol^{-1}. Taking this method dependence into consideration, the energy difference between **5** and **6** also amounts probably to 115 ± 15 kJ mol^{-1} in favour of **6**. Note also that the diol **5** lies about 29 kJ mol^{-1} higher in energy than the separated $C_3O_2 + H_2O$ reactants whose pre-association leads to various weak hydrogen-bonded complexes. Their complexation energies are calculated to be not larger than 10 kJ mol^{-1}. To simplify the presentation of data, they are not shown here. Note that the (C_3O_2·HCl) complex has recently been detected in matrix isolation experiments.[28,34]

Hydration of carbon suboxide by one water molecule. The nucleophilic attack of one water molecule across both C=O and C=C bonds of **1** is characterized by transition structures **TS1/CO** and **TS1/CC**, respectively, displayed in Fig. 2. For the purpose of comparison, the corresponding MP2/6–31G(d,p) parameters optimized for the ketene hydration[21a] are also given (values in italics). In both cases, the bending of the C_3O_2 skeleton around one ketene moiety is important, up to 50°. The other ketene moiety in C_3O_2 remains almost linear. Overall, the geometric characteristics of both transition structures **TS1/CC** and **TS1/CO** do not differ significantly from those of ketene, except for the fact that, in the C_3O_2 case, the cyclic structures become more compact, a sign of a later transition state.

Calculated energetic data related to the $C_3O_2 + H_2O$ reaction are summarized in Table 2. On the one hand, it is clear that the C=C addition via **TS1/CC** turns out to be more favored by 46 kJ mol^{-1} over the C=O process via **TS1/CO**. On the other hand, the energy barrier for the C=C addition appears to be substantial, being 164 kJ mol^{-1} at the QCISD/6–31G(d,p) level of accu-

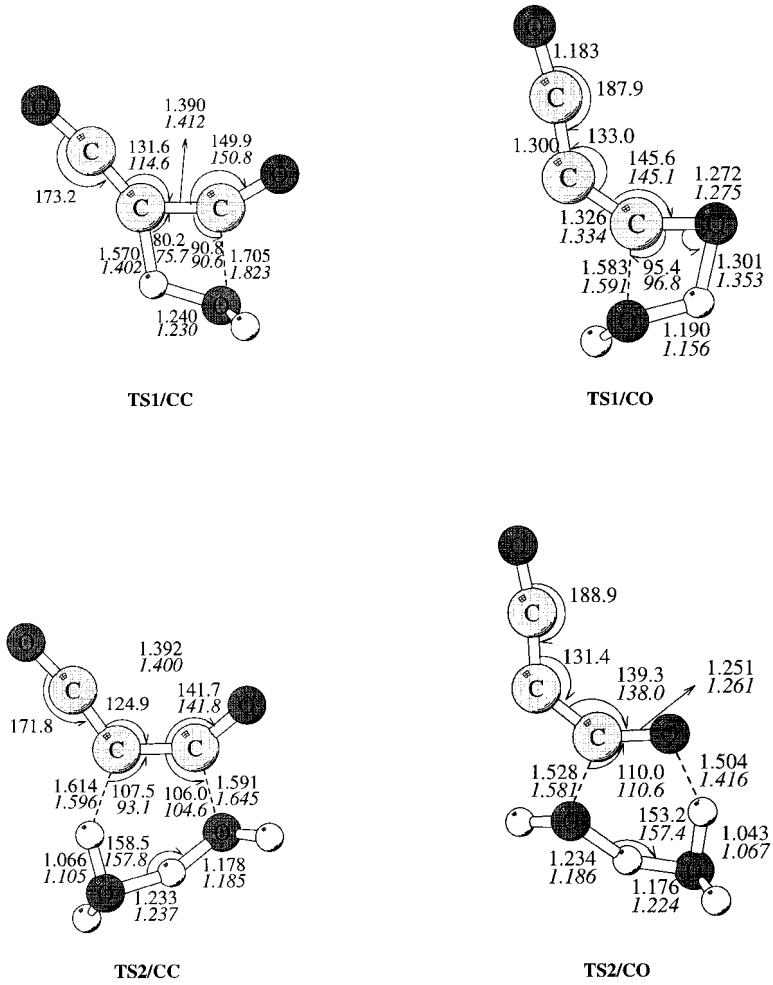

Figure 2. MP2/6–31G(d,p)-optimized geometries of the transition structures for addition of one and two water molecules across both C═O and C═C bonds of carbon suboxide. Values given in italics correspond to those of the ketene hydration

racy. Using the same method, the corresponding energy barriers for analogous hydration reactions are as follows (in kJ mol^{-1}): CO_2, C═O addition 214; $H_2C{=}C{=}O$, C═O addition 161 and C═C addition 170; and O═C═C═C═O, C═O addition 210 and C═C addition 164. Two significant points can be noted: (i) the energy barriers to C═C addition are comparable in two related systems, with a slight decrease from ketene to carbon suboxide; and (ii) in contrast, the energy barrier to C═O addition increases appreciably on going from ketene to carbon suboxide, by 49 kJ mol^{-1}; the barrier for C═O addition in ketene is the smallest of the three systems examined.

Hydration of carbon suboxide by water dimer. As mentioned in the Introduction, it has repeatedly been demonstrated that at least two water molecules should be employed to model the hydration reaction in aqueous solution.[19–22] This is in fact a classical example of an active solvent catalysis which sharply reduces the activation energies. For this case, we have been able to identify two distinct transition structures, **TS2/CO** and **TS2/CC**, whose geometric parameters are also shown in Fig. 2 along with the relevant values for the ketene hydration.[21a] As expected, the calculated energy barriers become strongly reduced in both additions (Table 3). The calculations show that as the energetically most favoured transition state **TS2/CC** is approached, the two molecules of water move in the form of a dimer towards carbon suboxide. Similarly to the one water case, the addition of two water molecules across the C═C bond of C_3O_2 appears to be favoured over that across the C═O bond, with values of 99 and 130 kJ mol^{-1}, respectively (at MP2 level of theory). In **TS2/CC** there are two important nuclear motions: the deformation of C_3O_2 [α(CCC) = 125°] and the closure of the OHO angle of the dimer from 179° to 158°. These movements tend to facilitate the transfer of a proton towards the C_β carbon. Whereas for C_3O_2 (**1**) the attack of water dimer across the C═C-bond is more favoured, the addition across the C═O bond is confirmed to be more probable for ketene.[22] At the highest calculated level (QCI), the

Table 3. Calculated total and relative energies of the points related to the addition of two water molecules to carbon suboxide, carbon dioxide and ketene

		Total Energies		Relative Energies[c]	
Species[a]	ZPE[b]	MP2/6–31G(d,p)	QCISD(T)/6–31G(d,p)	MP2/6–31G(d,p)	QCISD(T)/6–31G(d,p)
$C_3O_2 + 2\ H_2O$	166	−416.47283	—	0	—
TS2/CO	174	−416.41692	—	155	—
TS2/CC	173	−416.42826	—	124	—
$H_2C{=}C{=}O + 2\ H_2O$	190	−304.62119	−304.65858	0	0
$H_2CCO\ldots\ (H_2O)_2$ complex	205	−304.64538	−304.68223	−49	−47
TSCO	207	−304.61095	−304.64487	44	53
$H_2CCO\ldots\ (H_2O)_2$ complex	205	−304.64505	−304.68064	−48	−43
TSCC	207	−304.60914	−304.63990	48	66
$CO_2 + 2\ H_2O$	140	−340.56326	−340.58620	0	0
$CO_2\ldots\ (H_2O)_2$ complex	153	−340.58563	−340.60791	−45	−44
TSCO	153	−340.53498	−340.55595	87	92

[a] Based on MP2/6–31G(d,p) optimized geometries.
[b] From HF/6–31G(d,p) geometries and scaled by 0.9.
[c] At the indicated level and ZPE corrections.

energy barrier for attack across the C=C-bond is about 9 kJ mol^{-1} lower than the corresponding value for the C=C-bond.

Overall, inclusion of a second water molecule tends, as expected, to reduce the energy barrier dramatically in both C_3O_2 and $H_2C{=}C{=}O$ molecules, but does not change the fact that both cumulenes have different mechanisms concerning the addition of water. As mentioned above, the energy difference between the diol and acid isomers is similar in both cases. Thus the higher thermodynamic stability of the acid is an important but not predominant factor. The driving force is likely to reside in the ease with which carbon suboxide undergoes molecular distortion. Its lowest vibrational frequency is calculated to be 114 cm^{-1} (see above) and is associated with a bending motion of the carbon backbone. Such a

Table 4. Calculated total and relative energies of the points of interest on the addition path of a H_2, HF and HCl molecule to C_3O_2

				Relative energies[c]	
Structure[a]	ZPE[b]	MP2/6–31G(d,p)	QCISD(T)/6–31G(d,p)	MP2	QCISD(T)
C_3O_2 (**1**)	56	−264.02793	−264.03519	—	—
H_2	25	−1.15766	−1.16514	—	—
HF	24	−100.19464	−100.20128	—	—
HCl	17	−460.20545	−460.22196	—	—
$C_3O_2 + H_2$	81	−265.18559	−265.20033	0	0
OCCCHOH (**5H**)	108	−265.17254	−265.19680	61	36
OCCH-COH (**6H**- *cis*)	110	−265.21402	−265.23804	−46	−70
OCCH-COH (**6H**- *trans*)	102	−265.21314	−265.23771	−51	−77
TS C=O (**TSH/CO**)	86	−265.02812	−265.06642	418	357
TS C=C (**TSH/CC**)	83	−265.06255	−265.08206	325	313
$C_3O_2 + HF$	80	−364.22257	−364.23647	0	0
OCCCFOH (**5F**)	89	−364.20098	−364.22061	66	51
OCCH-COF (**6F**- *cis*)	93	−364.25556	−364.27568	−73	−90
OCCH-COF (**6F**- *trans*)	93	−364.25704	−364.27724	−78	−94
TS C=O (**TSF/CO**)	79	−364.12467	−364.16200	256	195
TS C=C (**TSF/CC**)	77	−364.16824	−364.18275	140	138
$C_3O_2 + HCl$	73	−724.23338	−724.25715	0	0
OCCCClOH (**5Cl**)	85	−724.20991	−724.23225	74	77
OCCH-COCl (**6Cl**- *cis*)	88	−724.26245	−724.28521	−61	−59
OCCH-COCl (**6Cl**- *trans*)	84	−724.26261	−724.28547	−66	−63
TS C=O (**TSCl/CO**)	82	−724.13792	−724.18555	260	197
TS C=C (**TSCl/CC**)	78	−724.16231	−724.21246	192	122

[a] Based on MP2/6–31G(d,p) geometries.
[b] From HF/6–31G(d,p) calculations and scaled by 0.9.
[c] At the indicated level with the 6–31G(d,p) basis and corrected for ZPEs.

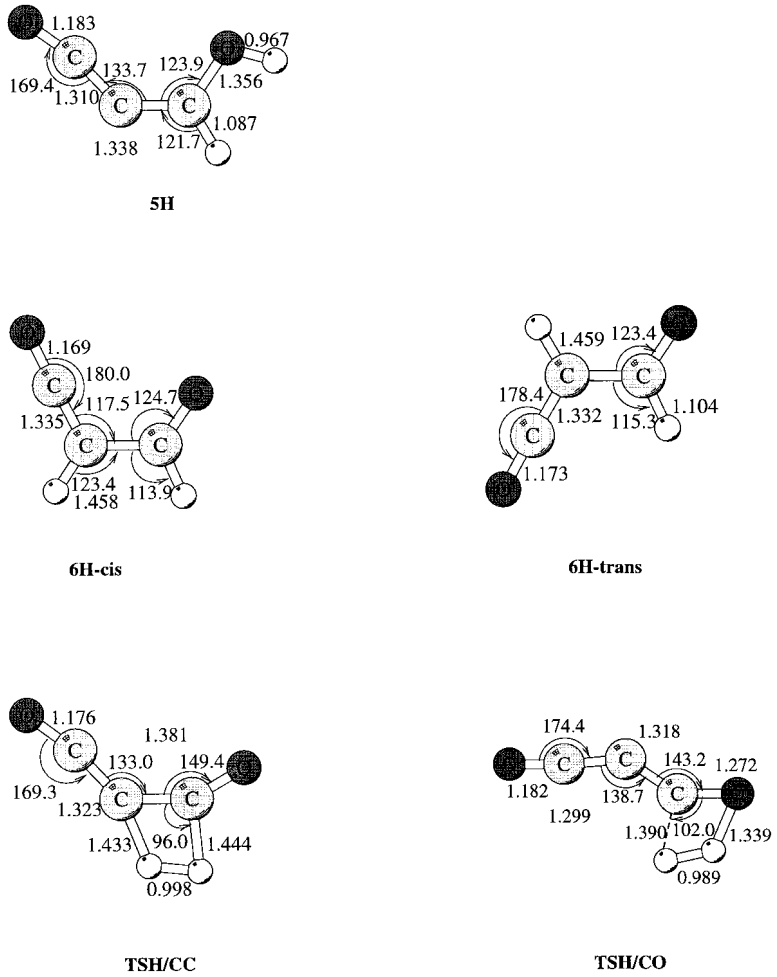

Figure 3. MP2/6–31G(d,p)-optimized geometries of stationary points for the addition of H_2 across both C═O and C═C bonds of carbon suboxide

nuclear deformation is much more facile to achieve than that of ketene, in particular in the TS for C═C addition which implies, in addition, a rotation of the terminal methylene group.[12]

Overall, the calculated results summarized in Table 3 suggest that the C═C addition in C_3O_2 is much more difficult to achieve than the C═O addition in ketene. The larger energy barrier for the former process is in line with the experimental observation[8] that the C_3O_2 hydration is much slower than the ketene.

In inspecting the geometric parameters of both transition structures **TS2/CC** and **TS2/CO**, it can be noted that the C—O bond formation is more advanced than either the C—H or the O—H bonding. In fact, the C—O distance varies from 1.59 Å in **TS2/CO** to 1.35 Å in **TS2/CC** to 1.36 Å in **6-*cis***, and from 1.53 Å in **TS2/CO** to 1.35 Å in **5**. In contrast, the C—H distance is 1.61 Å in **TS2/CC** and the O—H distance is 1.50 Å in **TS2/CO;** both are far longer than the corresponding equilibrium values. This fact is in line with the view that it is the nucleophilicity of the oxygen atom that actually leads the addition. Such a picture has been advanced before in terms of the reactivity of ketenes[3] and their selectivity towards substituted benzaldehydes.[35]

Addition of carbon suboxide to H_2, HCl and HF

In order to gain additional insight into the 1,2-addition of hydrogen compounds to carbon suboxide, the attacks of the simple hydrogen species H_2, HCl and HF across both the C═O and C═C bonds of **1** were also calculated and the results obtained are reported in Table 4. The corresponding stationary points are displayed in Figs 3, 4 and 5, respectively. The calculated values show that, similarly to the addition of H_2O, the attack across the C═C bond of C_3O_2 is inherently favoured. However, it should be noted that for the addition of H_2, both energy barriers across the C═O and C═C bonds are significantly higher than the corresponding values for the addition of HCl and HF. Such an ordering of barriers is in line with the stronger nucleophilic character of Cl in HCl and F in HF against H in H_2. Table 4 also shows that the activation energies for C═O addition of HF and HCl are

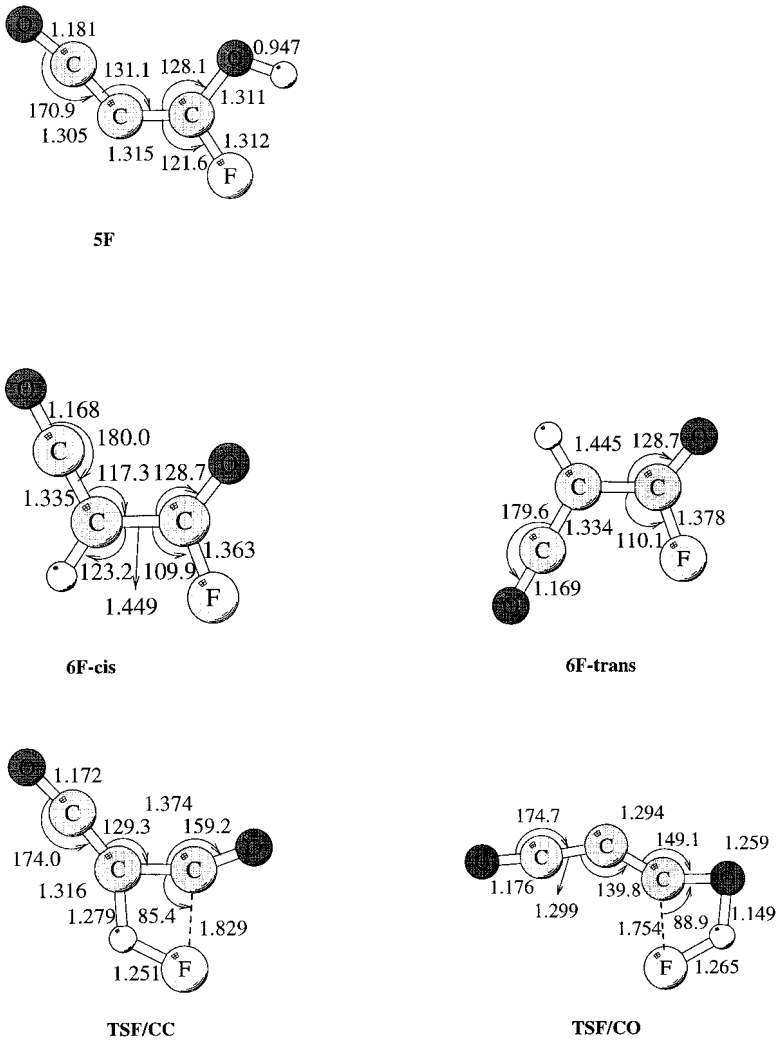

Figure 4. MP2/6–31G(d,p)-optimized geometries of stationary points for the addition of HF across both C═O and C═C bonds of carbon suboxide

similar (195 and 197 kJ mol^{-1}, respectively), whereas the energy barriers for C═C addition differ somewhat in favour of the HCl case, having an energy barrier of 122 kJ mol^{-1} against 138 kJ mol^{-1} for HF. Surprisingly, it seems that the geometry of the transition structure for attack of HCl, **TSCI/CC**, tends to be closer to its product than to the corresponding TS for HF, **TSHF/CC**. In **TSCI/CC** the C—H bond is almost formed (1.185 Å) whereas in **TSF/CC** the C—H bond is somewhat longer (1.279 Å) and its formation is less complete.

Furthermore, a plot of the molecular electrostatic potential (MEP) was made and is displayed in Fig. 6. The electronic charge distribution is indeed fundamental for understanding chemical reactivity and naturally allows the nucleophilic and electrophilic attacks to be explained on the basis of electrostatic interactions. However, the MEP gives information about the initial state of the molecule, whereas the change in electron density under the influence of an approaching reagent is also of importance. Moreover, a closer look at the charges on the different atoms in C_3O_2 (**1**) could not explain the preferred attack across its C═C bond. It is seen from the MEP in Fig. 6 that a proton would attack on O rather than on C_β. Fukui functions for both nucleophilic and electrophilic attacks have also been calculated. Whereas Fig. 6 shows the MEP of C_3O_2, Figs 7 and 8 display the Fukui functions, $f^{(+)}$ and $f^{(-)}$, calculated for **1**.

Depending on the type of attack, different sites are indicated as the most reactive site for C_3O_2, i.e. the site for which the Fukui function f is largest. The distinct mechanisms of hydration of **1** may illustrate this: the preferred attack is predicted to proceed via a nucleophilic attack of F^- on C_α [$f^{(+)}$ being largest for C_α and not for O, as can be seen from Fig. 7], whereas an electrophilic attack by a proton is suggested to occur by H^+ at the β-carbon [$f^{(-)}$ largest for C_β]. This indicates that the ability of the C_β atom to accept and distribute positive charge is of considerable importance, in such a way that the proton transfer to C_β is preferred. The polarizability feature is, of course, not contained in the MEP of the

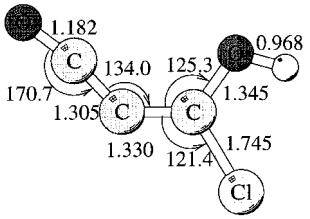

5Cl

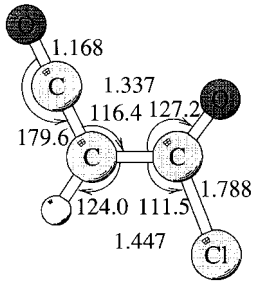

6Cl-cis

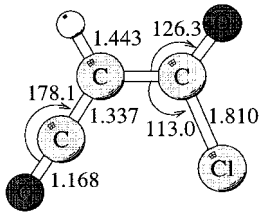

6Cl-trans

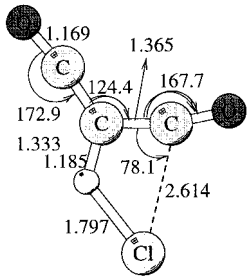

TSCl/CC

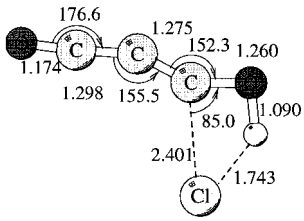

TSCl/CO

Figure 5. MP2/6–31G(d,p)-optimized geometries of stationary points for the addition of HCl across both C═O and C═C bonds of carbon suboxide

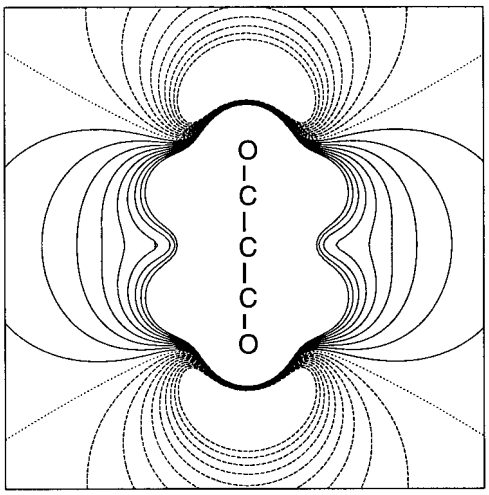

Figure 6. Contour plot of the molecular electrostatic potential (MEP) of C_3O_2 with the B3BW91/cc-pVTZ method. The solid isocontours correspond to positive potentials and the dashed lines to negative potentials

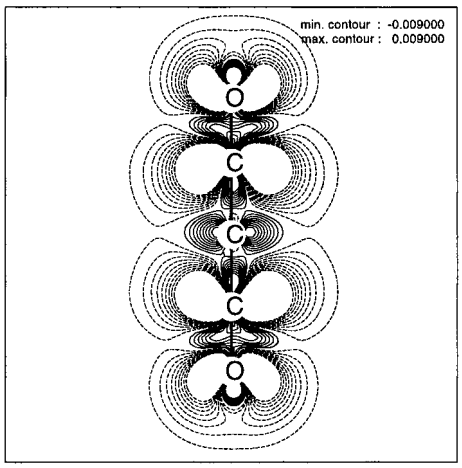

Figure 7. Contour plot of the Fukui function $f^{(-)}(r)$ for C_3O_2 with the B3PW91 method using the cc-pVTZ basis set. The solid isocontours correspond to positive values and the dashed lines to negative values of the $f(r)$ function

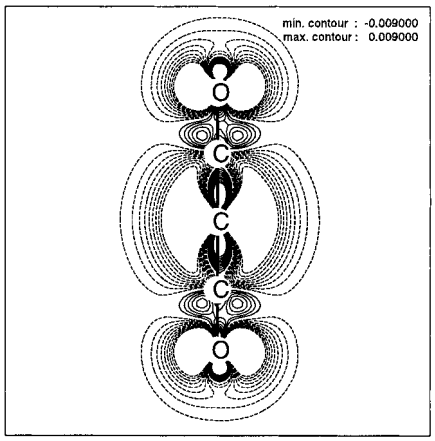

Figure 8. Contour plot of the Fukui function $f^{(+)}(r)$ for C_3O_2 with the B3PW91 method using the cc-pVTZ basis set. The solid isocontours correspond to positive values and the dashed lines to negative values of the $f(r)$ function

unperturbed initial state. It may therefore be concluded that the reactivity of C_3O_2 can better be rationalized in terms of Fukui functions.

The Fukui functions of the parent ketene ($H_2C{=}C{=}O$) have been analyzed in some detail in a recent paper.[21a] Accordingly, attack of water to ketene can occur either in the molecular plane (C=O) or in the perpendicular plane (C=C). The preferred attack in the molecular plane thus proceeds via a nucleophilic approach of O of water to C_α of ketene [having the largest $f^{(+)}$ value] and an electrophilic approach by H of water to O of ketene [having the largest $f^{(-)}$ value]. This indicates the higher ability of the ketene O atom to accept and to redistribute a positive charge and, as a consequence, the preferential proton transfer to O over C_β. In the perpendicular plane of ketene, an opposite trend has been observed. That is, electrophilic attack now occurs at C_β which, in this plane, has the largest $f^{(-)}$ value. Overall, the Fukui functions predict that whereas a C=O addition is favoured in the molecular plane of ketene, a C=C addition is preferred in its perpendicular plane. Of course, it is not obvious to interpret the activation energies, in order to differentiate both additions, solely on the basis of $f^{(-)}$ values. The Fukui functions are essentially static reactivity indices, and a general correlation between them and activation energies could not be established.[36–38]

In summary, the present theoretical study points towards an inherent difference in the addition mechanism of water, and most probably of hydrogen molecules, to carbon suboxide and ketene. Whereas a direct C=C addition is dominant in carbon suboxide, a two-step C=O addition is preferred in ketene. As carboxylic acids or related adducts are thermodynamically more stable than their enol isomers, the C=C addition appears to be intrinsically favoured. The reverse case observed in ketenes is simply due to a higher energy cost associated with a more severe molecular deformation in the transition states. The calculated results also confirm that the hydration of carbon suboxide is much slower than that of ketene. Fukui functions appear to be useful reactivity indices for rationalizing the preferential hydration reaction.

Acknowledgements

The authors are grateful to the Flemish science foundations FWO-Vlaanderen, IWT and GOA-program for continuing support.

REFERENCES

1. (a) T. Kappe and E. Ziegler, *Angew. Chem., Int. Ed. Engl.* **13**, 491 (1974); (b) O. Diels and B. Wolf, *Chem. Ber.* **89**, 689 (1956); (c) H. Staudinger and S. Bereza, *Chem. Ber.* **41**, 4462 (1888).
2. (a) T. Kappe, *Methoden der Organische Chemie*, Vol. E15. Georg Thieme, Stuttgart (1993); (b) S. Polanc, M. C. Labillw, Z. Janousek, R. Merenyi, M. Verimander, H. G. Viehe, B. Tinant, J. Piret-Meunier and J. P. Declercq, *New J. Chem.* **15**, 79 (1991).
3. T. T. Tidwell, *Ketenes*, Chapt. 4, p. 434. Wiley, New York (1995).
4. M. L. Burke, W. L. Dimpfl, P. M. Schaefer, P. F. Zittel and L. S. Berstein, *J. Phys. Chem.* **100**, 138 (1996).
5. W. T. Huntress, M. Allen and A. Delisley, *Nature (London)* **352**, 316 (1991).
6. C. E. M. Strauss, S. H. Kable, G. K. Chawk, P. L. Houston and I. R. Burak, *J. Chem. Phys.* **94**, 1837 (1991).
7. H. Ulrich, *Cycloaddition Reactions of Heterocumulenes*, Chapt. 3, p. 110. Academic Press, New York (1963).
8. A. D. Allen, M. A. McAllister and T. T. Tidwell, *J. Chem. Soc., Chem. Commun.* 2547 (1995).
9. (a) J. Andraos and A. J. Kresge, *J. Photochem. Photobiol. A* **57**, 165 (1991); (b) E. Bothe, A. M. Dessouki and D. Schulte-Frohlinde, *J. Phys. Chem.* **84**, 3270 (1980).
10. G. Bouchoux and Y. Hoppillard, *J. Phys. Chem.* **92**, 5869 (1988).
11. M. T. Nguyen, D. Sengupta, G. Raspoet and L. G. Vanquickenborne, *J. Phys. Chem.* **99**, 11883 (1995).
12. M. T. Nguyen and A. F. Hegarty, *J. Am. Chem. Soc.* **106**, 1552 (1984).
13. M. T. Nguyen and P. Ruelle, *Chem. Phys. Lett.*, **138**, 486 (1987).
14. (a) J. Andraos and A. J. Kresge, *J. Mol. Struct. (Theochem)* **233**, 165 (1991); (b) J. Andraos, A. J. Kresge, M. R. Peterson and I. G. Csizmadia, *J. Mol. Struct. (Theochem)* **232**, 155 (1991); (c) P. N. Skancke, *J. Phys. Chem.* **96**, 8065 (1992).
15. B. M. Allen, A. F. Hegarty, P. O'Neill and M. T. Nguyen, *J. Chem. Soc., Perkin Trans. 2*, 927 (1992).
16. B. Urwyler and J. Wirz, *Angew. Chem., Int. Ed. Engl.* **29**, 790 (1990).
17. (a) Y. Chiang, A. J. Kresge, P. Pruszinski, N. P. Schepp and J. Wirz, *Angew. Chem., Int. Ed. Engl.* **29**, 792 (1990); (b) J. Andraos, Y. Chiang, A. J. Kresge and V. V. Popik, *J. Am. Chem. Soc.* **119**, 8417 (1997).
18. J. Frey and Z. Rappoport, *J. Am. Chem. Soc.* **117**, 1161 (1995).
19. M. T. Nguyen and A. F. Hegarty, *J. Am. Chem. Soc.* **105**, 3811 (1983).
20. M. T. Nguyen and T. K. Ha, *J. Am. Chem. Soc.*, **106**, 599 (1984).
21. (a) M. T. Nguyen and G. Raspoet, *Can. J. Chem.* **77**, 817 (1999); (b) G. Raspoet, M. T. Nguyen, M. McGarraghy and A. F. Hegarty, *J. Org. Chem.* **63**, 6867 (1998); (c) G. Raspoet, M. T. Nguyen, M. McGarraghy and A. F. Hegarty, *J. Org. Chem.* **63**, 6878 (1998); (d) G. Raspoet, M. T. Nguyen, S. Kelly and A. F. Hegarty, *J. Org. Chem.* **63**, 9669 (1998).
22. M. T. Nguyen, G. Raspoet, L. G. Vanquickenborne and P.Th. Van Duijnen, *J. Phys. Chem. A* **101**, 7379 (1997).
23. M. J. Frisch, G. W. Trucks, H. B. Schlegel, P. M. W. Gill, B. G. Johnson, M. A. Robb, J. R. Cheeseman, T. Keith, G. A. Petersson,

J. A. Montgomery, K. Raghavachari, M. A. Al-Laham, V. G. Zakrzewski, J. V. Ortiz, J. B. Foresman, J. Cioslowki, B. B. Stefanov, A. Nanayakkara, M. Challacombe, C. Y. Peng, P. H. Ayala, W. Chen, M. W. Wong, J. L. Andres, E. S. Replogle, R. Comperts, R. L. Martin, D. J. Fox, J. S. Binkley, D. J. DeFrees, J. Baker, J. J. P. Stewart, M. Head-Gordon, C. Gonzalez and J. A. Pople, GAUSSIAN 94, Revision C.3. Gaussian, Pittsburgh, PA (1995).
24. R. G. Parr and W. Yang, *Density Functional Theory of Atoms and Molecules*. Oxford University Press, New York (1989).
25. P. Geerlings, F. De Proft and J. M. L. Martin, *Recent Developments and Applications of Modern Density Functional Theory*, Vol. 4. Elsevier, Amsterdam (1996).
26. P. Brown, R. Champion, P. S. Elmes and P. D. Godfrey, *J. Am. Chem. Soc.* **107**, 4109 (1985).
27. P. Jensen and J. W. C. Johns, *J. Mol. Spectrosc.* **118**, 248 (1986).
28. N. Pietri, T. Chiavassa, A. Allouche, A. Rajzmann and J. P. Aycard, *J. Phys. Chem.* **100**, 7034 (1996).
29. S. G. Lias, J. E. Bastmess, J. F. Liebman, J. L. Holmes, R. Levin and W. G. Mallard, *J. Phys. Chem. Ref. Data* **17**, Suppl. 1 (1988).
30. J. C. Traeger and B. M. Kompe, *Org. Mass Spectrom.* **26**, 289 (1991).
31. G. Bouchoux and J. Y. Salpin, *J. Phys. Chem.*, **100**, 16555 (1996).
32. D. M. Birney, *J. Org. Chem.* **59**, 2557 (1994), and references cited therein.
33. M. T. Nguyen, T. K. Ha and R. A. More O'Ferrall, *J. Org. Chem.* **55**, 3251 (1990).
34. N. Pietri, T. Chiavassa, A. Allouche and J. P. Aycard, *J. Phys. Chem. A* **101**, 1093 (1997).
35. S. Ham and D. M. Birney, *Tetrahedron Lett.* **38**, 5925 (1997).
36. A. K. Chandra and M. T. Nguyen, *J. Chem. Soc., Perkin Trans. 2* 1415 (1997).
37. A. K. Chandra, M. Michalak, M. T. Nguyen and R. F. Nalewajski, *J. Phys. Chem. A* **102**, 10182 (1998).
38. A. K. Chandra and M. T. Nguyen, *J. Phys. Chem. A* **102**, 6181 (1998).

